Interaction between Refractory Crucible Materials and the Melted NiTi Shape-Memory Alloy

S.K. SADRNEZHAAD and SADEGH BADAKHSHAN RAZ

Attempts have been made to quantify the amount of contaminants absorbed by liquid metal from commercial ZrO_2-, Al_2O_3-, and SiC-base crucibles used for vacuum melting of Ni-45 wt pct Ti alloy. The molten alloy was held under vacuum for 90 minutes at 1450 °C to become homogenized. Reactions between the liquid metal and the crucible were investigated by visual observation, chemical analysis, scanning electron microscopy (SEM) image processing, and X-ray mapping. The relative degree of contamination declined in the following sequence: commercially pure SiC > SiC-5 wt pct Al_2O_3-5 wt pct SiO_2 > slurry cast alumina > recrystallized alumina > zircon type A > oxygen deficient high-purity zirconia. Thermodynamic calculations showed a difference between the equilibrium and the experimental data, indicating that except for commercially pure SiC crucible, the amount of the crucible elements entering the melt is greater than the calculated equilibrium values. This discrepancy seems to be due to the immersion into the melt of the undissolved chemical compounds formed due to the reactions between the crucible and the liquid phase.

I. INTRODUCTION

EXCELLENT shape memory, superelasticity, and mechanical properties have introduced NiTi as an extremely useful family of newly developed alloys. These properties depend greatly on the exact chemical composition, processing history, and smallness of undesirably dissolved elements.[1] Contaminants such as oxygen and carbon can dramatically affect the properties of the NiTi shape memory alloy. Their penetration occurs basically during production and processing of the alloy.

Commercial production processes usually involve induction melting of the alloy under heavy vacuum. A major source of contaminants is the melting crucible, which needs to be carefully chosen. Numerous investigators[2,3,4] have tried to solve the problem, but they have generally not been able to obtain a satisfying result, because the contaminating behavior of the ordinary materials (oxides, borides, silisides, sulfides, nitrides, fluorides, Mo_3Al, and W) could never be totally stopped.

In an early study, zirconia stabilized with titanium was found to be the least reactive one.[2] Later investigators[4,5] indicated that Y_2O_3 performs even better than ZrO_2. Other investigators[5] indicated that Y_2O_3 stabilized with 8 to 15 wt pct of titanium has the best performance. Yttria is, however, fairly expensive, which is a drawback.

Induction and arc skull melting processes both were used to prevent the molten metal contamination. These processes possessed, however, very low energy efficiency and great difficulty in obtaining sufficient superheats generally needed for a better molten metal homogenization.[6]

In order to improve the quality of NiTi casting objects and reduce the production costs, it is, therefore, necessary to introduce a refractory material capable of melting highly reactive NiTi alloys. The present study deals with quantification of instability and contamination formation behavior of various refractory crucibles in order to help the development of low cost materials such as zirconia, alumina, and silicon carbide for melting of the NiTi shape memory materials.

S.K. SADRNEZHAD, Professor, and SADEGH BADAKHSHAN RAZ, Research Assistant, are with the Department of Materials Science and Engineering, Sharif University of Technology, P.O. Box 11365-9466, Teheran, Iran. Contact e-mail: sadrnezh@yahoo.com or sadrnezh@sharif.edu

Manuscript submitted January 17, 2003.

II. EXPERIMENTS

A. *Melting Procedure*

High content zirconia, zircon type A (ASTM C574-70), recrystallized alumina, slurry cast alumina, commercially pure SiC, and SiC-$5Al_2O_3$-$5SiO_2$ commercial crucibles with chemical compositions given in Table I were used in this investigation.

For evaporation of the absorbed humidity, all crucibles were heated to 200 °C ± 10 °C in a resistance furnace and wrapped with a piece of aluminum foil in order to prevent the possible re-absorption of humidity. The interaction between the crucibles and the melt was studied in a vacuum resistance furnace with heating elements made of tungsten. The chemical composition of the charge material was Ni-45 wt pct Ti. After placing the crucible inside the chamber and evacuating the chamber for up to 10^{-6} mbar, electric heating was started. The temperature of the crucible was gradually increased up to 1450 °C, *i.e.*, 140 °C above the melting point of NiTi (1310 °C). Although soaking for 30 minutes at this temperature was adequate, the specimens were held molten for 90 minutes to become homogenized in terms of temperature and composition. Subsequent cooling decreased the temperature of the specimen down to the room temperature while vacuum was maintained at 10^{-6} mbar.

B. *Inspection of the Melted Samples*

Various methods were used to evaluate the interaction of the molten metal with the refectory materials of the crucible holding the melt. Visual observations were accomplished right after separating the solidified specimen from the crucible by a diamond-disk cutter. The specimens were then mounted for

the mechanical removal of a 0.3-mm-thickness layer from the surface of the solidified melt. Particle-induced X-ray spectroscopy (PIXE) was used to determine the chemical analyses of the specimens. The specimens were bombarded with fast protons having energy of 2 MeV. The areas affected with the proton beam had a diameter of 2 mm. In order to detect the heavy elements such as zirconium, a miller filter with 175-μm thickness was used. Scanning electron microscopy (SEM) was used to evaluate the microstructure of the melted specimens. The distribution of the species dissolved from the crucible into the melt was also determined by X-ray mapping. A Vickers indicator with a load of 1.4 kg was used to measure the average hardness of the melted specimens.

Table I. Chemical Compositions (Weight Percent) of the Crucibles Used in This Study

Crucible Type	ZrO_2	SiO_2	Al_2O_3	SiC	Others
Recrystallized Alumina	—	—	99.5	—	0.5
Slurry cast Alumina	—	—	99	—	1
High content Zirconia	93.7	5.3	—	—	1
Zircon type A	66	33	—	—	1
SiC-Al_2O_3-SiO_2	—	5	5	90	—
CP SiC	—	—	—	99	1

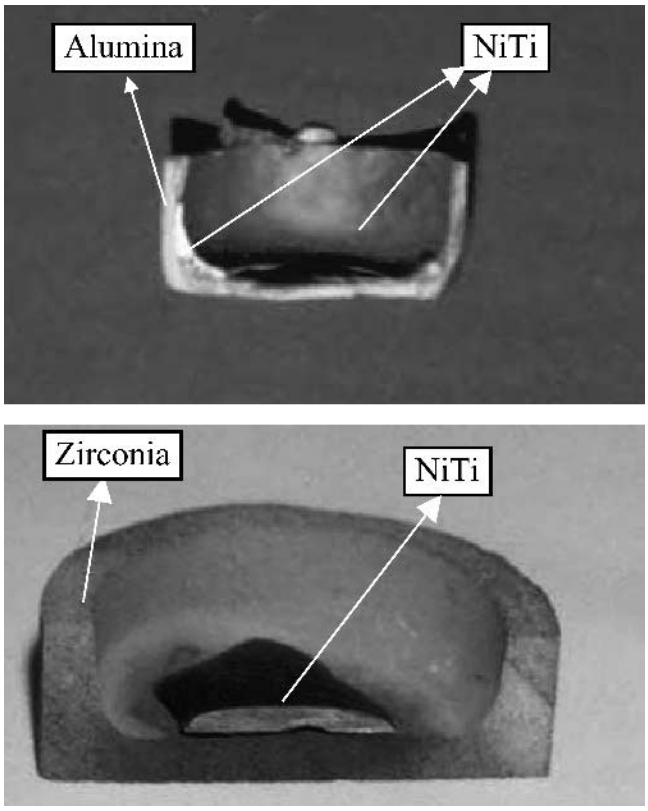

Fig. 1—Picture of melted specimen in recrystallized alumina crucible (top) and melted specimen in high content zirconia crucible (bottom).

III. RESULTS AND DISCUSSION

A crucible wetting with the melt is an indication of a mild reaction that may occur between the molten metal and the crucible. A concave meniscus visually observed after solidification of the melt evidences wetting. A convex meniscus proves, however, that no contamination has occurred.[2] Previous researchers have observed that the dissolution of the refractory materials into the melt is a common case.[3]

Specimens melted in high content zirconia showed convex meniscus, *i.e.*, no crucible wetting. Specimens melted in zircon type A crucibles indicated poor wetting. All other crucibles indicated concave menisci, *i.e.*, they were wetted with the melt.

Figure 1 illustrates photographs of the specimens melted in high content zirconia and recrystallized alumina-type crucibles. The results indicated that SiC and alumina base crucibles were completely wetted with the melt. So the interaction of these crucibles with the melt was greater than that of the zirconia-based crucibles.

Chemical compositions of the specimens were analyzed by the PIXE method. Table II summarizes the results indicating that there is less titanium in the solidified specimens than the initially charged values. The discrepancies are due to (1) the formation of titanium-rich chemical scurf at the crucible/metal interface and its subsequent removal by grating and ablation during the specimen preparation, (2) titanium oxidation, (3) titanium evaporation, (4) alloy wetting of the crucible, and (5) alloy penetration into the crucible. Because of the relatively high initial surface to volume ratio of the sample (7.1 cm^2/1.5 cm^3) and the increasing effects of the alloy wetting and penetration, the influences of the titanium-consuming reactions are magnified in the relatively small samples used in this investigation and the losses of titanium cannot be assumed negligible.

As is indicated, all crucibles dissolve to some extent into the Ni-45 wt pct Ti melt. Figure 2 illustrates a typical example. The amount of dissolution depends on both thermodynamics and kinetics of the process. Some insoluble particles may also mechanically enter into the melt. A long holding time can, however, cause them to float away. A short holding time after the entrance can simply cause the crucible particles to immerse inside the melt. The infected

Table II. Chemical Analyses of Specimens Determined by the PIXE Method *vs* the Crucible Type (Weight Percent)

Crucible Type	Ti Pct	Si Pct	Zr Pct	Al Pct	C Pct	O Pct	Ni Pct
Recrystallized alumina	37.554	—	—	1.800	—	1.600	bal
Slurry cast alumina	41.733	—	—	1.799	—	1.600	bal
High content zirconia	40.423	0.908	0.007	—	—	1.046	bal
Zircon type A	40.873	1.635	0.005	—	—	1.872	bal
Pure SiC	41.566	1.887	—	—	1.129	—	bal
SiC-Al_2O_3-SiO_2	41.286	2.614	—	0.106	1.448	0.744	bal

areas, however, are close to the metal crucible interface. The composition of the melt consisting both of the dissolved and the suspended particles may exceed the equilibrium values in such a case.

Detailed investigations—made with SEM and X-ray diffraction—of the composition of the solidified specimens at different locations indicated different amounts of contamination caused by use of alternative crucibles. Figure 3 illustrates SEM images and X-ray maps of the silicon scattered in the specimens melted in zircon type A and commercial pure SiC holding crucibles.

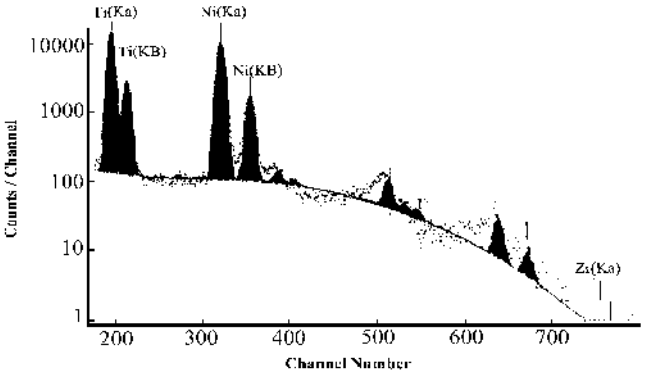

Fig. 2—Result of chemical analysis of specimen melted in high content zirconia crucible determined by PIXE method (Miller filter is used).

It was found that the specimen melted in the zircon type A had an approximately flat surface, while the specimen melted in the commercially pure (CP) SiC crucibles had a porous spongy surface. This indicated that NiTi melts interacted more vigorously with the CP SiC crucibles than they did with the zircon type A's.

X-ray maps confirmed the preceding effect by indicating that the crucible elements such as Al, Si, Zr, C, and O dissolve from all types of crucibles into the liquid phase to some extent. A typical example is shown in Figure 3. Similar results indicated that higher average hardness of at least 2 points in Vickers scale was achieved when the specimens were made of the alloys melted in the CP SiC crucibles (Figure 4).

The data obtained from visual observations, chemical analyses, SEM images, X-ray maps, and hardness tests were all consistent in showing the following sequence for reduction of the crucible contaminating effects due to the crucible dissolving process:

CP SiC > SiC-Al_2O_3-SiO_2 > slurry cast alumina recrystallized alumina > zircon type A > high content zirconia

These results showed that pure zirconia-type crucibles were the most stable ones, while the SiC base crucibles were the least stable ones. The low stability of the SiC base crucibles

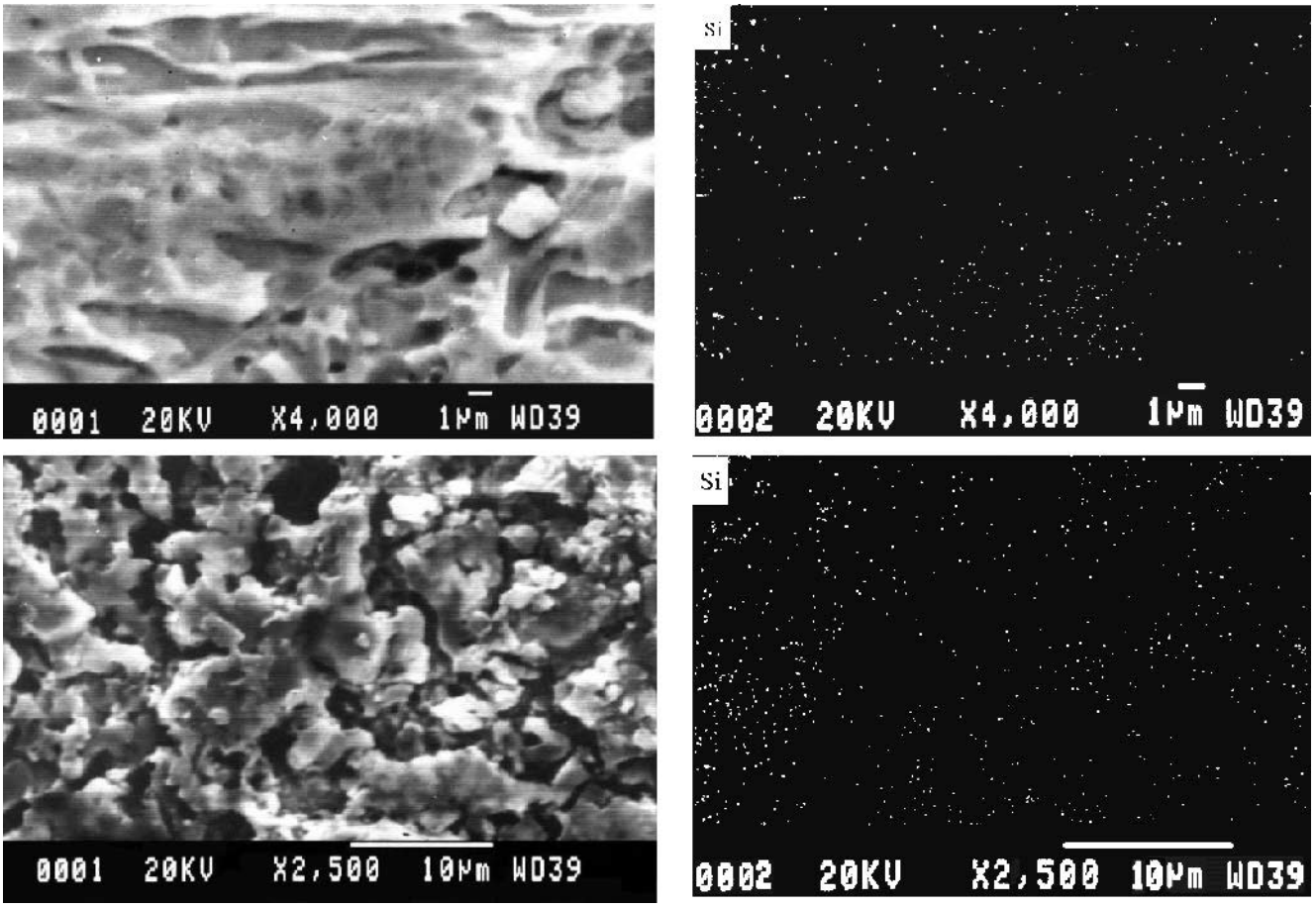

Fig. 3—SEM images (left) and X-ray maps (right) of Si dissolved into NiTi melted specimen in high content zirconia (top) and commercial pure SiC crucibles (botom).

can be explained by Gibbs free energy changes of the dissociative dissolution reactions. The standard Gibbs free energy changes of the dissociative dissolution reactions are shown for SiC in nickel-base melts in Table III. It is seen that the standard Gibbs free energy changes of the dissociative dissolution reactions of alumina and zirconia in nickel-base melts are positive, while the standard Gibbs free energy change of the dissociative dissolution reaction of SiC in nickel base melts is negative. Although this result is consistent with the relatively low stability of the SiC crucibles as compared to that of the high alumina and zirconia ones, the activities of the species of the reaction must also be taken into consideration. The actual activities of the species present in different reaction interfaces are, thus, a matter of significant importance and concern.

Other factors such as wetability and penetration also need to be taken into consideration in order to obtain a more realistic picture. As an example, the standard Gibbs free energy change of the dissociative dissolution reaction of zirconia is less than that for alumina (Table III), while according to the experimental results, the stability of zirconia-based crucibles is greater than that for alumina. The results of visual inspection, however, showed that the alumina- and SiC-base crucibles were completely wetted by the melt, but zircon type A and high content zirconia crucibles were poorly wetted with the melt (Figure 1). It can, therefore, be concluded that the zirconia-based crucibles have lower tendency for wetting with Ni-45 wt pct Ti melts. The weight percent of SiO_2 in high content zirconia crucibles is 5.3 pct, while that of zircon type A is 33 pct. The larger amount of ZrO_2 in high content zirconia crucibles causes poorer wetting of the crucible. These observations support the earlier findings that the zirconia-based crucibles possess a lower wetting tendency when encountered with the rich titanium melts.[2] The poor wetting of the crucibles with the melt retards their dissolution kinetics and causes a less destructive effect.

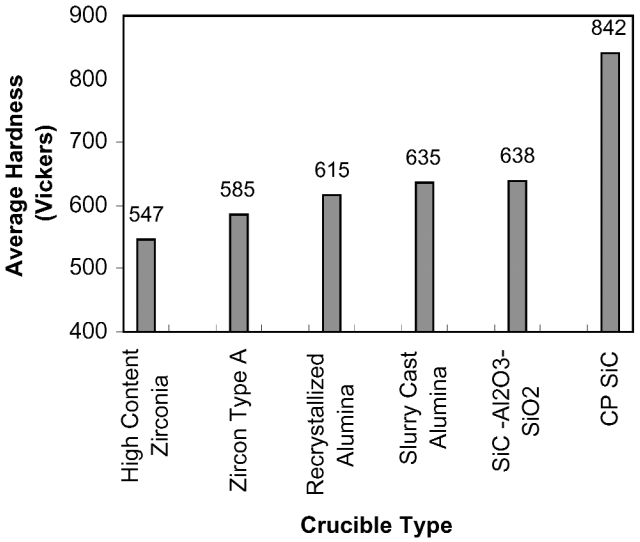

Fig. 4—Average hardness of the specimens melted in different refractory crucibles.

The zirconia-based crucibles are usually used for melting of nickel-based alloys.[7] Earlier investigators[2] have shown that the zirconia-based crucibles could be used for melting titanium alloys with lower contaminations absorbed by the melt. Due to their lower titanium content, the reactivity of the molten shape memory alloys is less than that of CP titanium or other titanium-rich alloys. The melting point of the former is lower than that of the latter. These results indicate that using the zirconia-based crucibles for production of NiTi shape memory alloy must be preferred to other specified crucibles.

Observations showed that oxygen is a serious contaminant generally present in the melt (Table I). A careful study indicates that the amount of Zr is negligible in the melt showing that the important source of oxygen contaminant is SiO_2, while ZrO_2 is a relatively stable constituent of the crucible refractory material. Oxygen deficient zirconia crucibles, therefore, seem to be desirable for melting of NiTi-based shape memory alloys. These types of crucibles can be produced by utilization of stabilizing agents such as titanium.[2] Zirconia crucibles having plasma-sprayed yttria coatings can also be recommended for melting of NiTi-based shape memory alloys, because of the excellent chemical stability of the latter.[5,6]

A. *Thermodynamics of Melt-Crucible Reactions*

Thermodynamic calculations have been carried out in order to assess the equilibration between the crucible and the NiTi liquid alloy held inside the crucible for 90 minutes. The procedure is similar to that used by Coach[9] and Saha *et al.*,[8] who have evaluated the decomposition dissolution of Y_2O_3[8] and ZrO_2[9] crucibles containing titanium melt.

Table III. Standard Gibbs Free Energy Changes of Reactions Taking Place in this Study

Reaction	ΔG° (in kcal) at 1723 K	Reference
$<Al_2O_3> \rightarrow 2\{Al\} + 3/2\,(O_2)$	268	9
$<ZrO_2>_\beta \rightarrow <Zr>_\beta + (O_2)$	182	9
$<SiC> \rightarrow \{Si\} + <C>$	11	9
$<Zr>_\beta \rightarrow \{Zr\}$	0.9	9
$\{Zr\} \rightarrow [Zr]_{1wt\ pct\ in\ nickel}$	−57	10
$\{Al\} \rightarrow [Al]_{1wt\ pct\ in\ nickel}$	−44	10
$\{Si\} \rightarrow [Si]_{1wt\ pct\ in\ nickel}$	−47	10
$<C> \rightarrow [C]_{1wt\ pct\ in\ nickel}$	−99	10
$1/2(O_2) \rightarrow [O]_{1wt\ pct\ in\ nickel}$	−16	10
$<Al_2O_3> \rightarrow 2[Al]_{1wt\ pct\ in\ nickel} + 3[O]_{1wt\ pct\ nickel}$	130	—
$<ZrO_2>_\beta \rightarrow [Zr]_{1wt\ pct\ in\ nickel} + 2[O]_{1wt\ pct\ nickel}$	93	—
$<SiC> \rightarrow [Si]_{1wt\ pct\ in\ nickel} + [C]_{1wt\ pct\ nickel}$	−46	—

Let's define a thermodynamic function called solubility function (F) similar to those used by the afore mentioned authors and determine its value both experimentally and theoretically. The closeness of these values is then considered as a criterion for assessment of the equilibrium conditions.

For the chemical reaction occurring between the melt and the crucible, we can consider the following general form:[3,8]

$$I_xJ_y \rightarrow x[I] + y[J] \quad [1]$$

in which I_xJ_y is the crucible species that dissolves in the melt, [I] indicates the dissolved state of the element I, and [J] is the other species that forms due to the dissociation-dissolution reaction. Under high vacuum, the following decomposition reaction can take place in the zirconia-based crucibles as well:[12,13]

$$ZrO_2 \rightarrow ZrO_{2-x} + x[O] \quad [2]$$

Due to the lake of the thermodynamic data available for equilibrium calculations, however, Eq. [2] is ignored by most researchers estimating the crucible solute contamination.[10] At equilibrium, the Gibbs free energy change of Reaction [1] is zero; hence,

$$\Delta G_1^\circ + R \times T \times \ln\left[\frac{(a_I)^x \times (a_J)^y}{(a_{I_xJ_y})}\right] = 0$$

Or

$$(a_I)^x \times (a_J)^y = (a_{I_xJ_y}) \times \exp\left(\frac{-\Delta G^\circ_I}{R \times T}\right) \quad [3]$$

where a indicates the activity of an element or compound and ΔG° is the standard Gibbs free energy change of the reaction. The standard Gibbs free energy changes of the reactions occurring between the crucible and the melt are given in Table III. Pure-stable materials are used as standard states of the components of the reactions, unless otherwise mentioned.

For activity of the element I dissolved in the melt, one can write

$$a_I = f_I(\text{wt pct I}) \quad [4]$$

where f_I is the activity coefficient of I being defined as follows:[10]

$$\log f_I = \sum_2^n (e_I^K \times [\text{wt pct K}]) + \sum_2^n (r_I^K \times [\text{wt\% K}]^2) \quad [5]$$

where e_I^K and r_I^K are the first- and the second-order interaction parameters of the element K on the element I, respectively. Because of the lack of the data on the interaction parameters of the elements dissolved in the nickel-base alloys, the first- and second-order interaction parameters were calculated from the quasi-chemical model developed for the solutions. According to the model, the interaction parameters were first calculated for the Raoultian standard state. They were then converted into the dilute-solution weight percent standard state. The first-order interaction parameter of the element I on I in the former standard state can, thus, be expressed as[10,14]

$$\varepsilon_I^I = Z \times [1 - (\gamma_I^\circ)^{\frac{2}{Z}}] \quad [6]$$

where Z is the coordination number of the element I and γ_I° is the Henry's constant of the element I in the 1-I system in which 1 is the base element of the solution. X-ray or neutron-ray diffraction methods have been used to determine the coordination number of the elements in the liquid state.[8,15–17] Few practical data, however, have been published for coordination numbers of the alloying elements used in this study. Previous researchers have assumed an approximate value of 10 for the coordination number of the alloying elements dissolved into the nickel-, cobalt-, or iron-base alloys.[9] Therefore, we used this value for the coordination number of the alloying elements used in this study. Henry's constants of these elements were also assumed to be equal to those in the nickel-base melts (Table IV). With these two assumptions, the first interaction parameters were, then, calculated for 1873 K. In order to calculate the interaction parameters of the elements at 1723 K, the following formula was employed:[10]

$$\varepsilon_I^K(T) = Z \times \left\{1 - \left[1 - \frac{\varepsilon_I^K(1873\text{ K})}{Z}\right]^{\frac{1873}{T}}\right\} \quad [7]$$

The value of ε_I^K (first-order interaction parameter of K on I in Raoultian standard state) can be calculated by the following formula:[10,15]

$$\varepsilon_I^K(T) = Z \times \left[1 - \sqrt{\frac{\left(1 - \frac{\varepsilon_I^I}{Z}\right) \times \left(1 - \frac{\varepsilon_K^K}{Z}\right)}{\left(1 - \frac{\varepsilon_I^I}{Z_K}\right)_{I-K}}}\right] \quad [8]$$

The formula for the second interaction parameter of K on I is as follows:[10,15]

$$\rho_I^K = \frac{1}{2Z}(\varepsilon_I^K)^2 + \frac{\varepsilon_K^K}{Z}\left(\varepsilon_I^K - \frac{Z}{2}\right) \quad [9]$$

where ρ_I^K is the second interaction parameter of K on I in the Raoultian standard state. For converting the first-order interaction parameter from the Raoultian standard state to dilute weight percent standard state, the following formula was used:[10]

$$e_I^K = \left(\varepsilon_I^K - \frac{M_1 - M_K}{M_1}\right) \times \frac{M_1}{230 \times M_K} \quad [10]$$

where M_1 and M_K are the molecular weights of the base and the K elements, respectively, and e_I^K is the first-order interaction parameter in the dilute weight percent standard state. For calculation of the second-order interaction coefficients in the dilute weight percent standard state, the following formula was used:[10]

Table IV. Henrian Activity Coefficients of the Elements Dissolved in a Nickel-Based Alloy at 1600 °C

Dissolved Element (i)	Henry's Constant at 1873 K	Reference
Al	0.00025	10
C (graphite)	0.32	10
$^1/_2O_2$	0.000187	11
Si	0.00014	10
Ti	0.00019	10
Zr	0.00005	10

$$r_I^K = \left\{ \left[\rho_I^K - \frac{1}{2} \times \left(\frac{M_1 - M_K}{M_1} \right)^2 \right] \times \frac{M_1^2}{230} - M_K \times (M_1 - M_K) \times e_I^K \right\} \times \frac{1}{100 \times M_K^2}. \quad [11]$$

where r_I^K is the second-order interaction parameter of K on I in the dilute weight percent standard state. Employing the preceding formulas, a computer program was developed to calculate the interaction parameters of the system. The values of the first- and the second-order interaction parameters thus calculated are given in Tables V and VI. Applying these data into Eq. [4] and [5] the activity coefficients of the elements dissolved in the melt were evaluated against the chemical composition of the melt.

For simplicity, let's abbreviate the weight percentages of the elements as

wt pct Al = A, wt pct Zr = Z, wt pct O = O, wt pct C = C and wt pct Si = S

Substituting these values into Eqs. [3] and rearranging all solute concentration terms to the left and other terms to the right-hand side of the equation, a relationship is obtained for evaluation of the solubility function (F) against other terms like Gibbs free energy change of the reaction. A typical example is Eq. [12], which illustrates the dissolution of the alumina-based crucible into the melt:

$$(2 \log A + 0.5A^2 - 3.57A) + (3 \log O + 0.976 O^2 - 4.188 O) = -[0.1053 (\text{wt pct Ti})^2 - 1.731 (\text{wt pct Ti})] + \log (a_{Al_2O_3}) + \log \left[\exp \left(\frac{-\Delta G^\circ}{R \times T} \right) \right] \quad [12]$$

Table V. Calculated First-Order Interaction Parameters in 1 Weight Percent Standard State at 1723 K

J→ / I↓	Ti	Si	Zr	Al	O	C
Ti	0.044	−0.015	0.021	0.038	−1.783	−0.035
Si	−0.007	0.077	0.018	0.06	−12.03*	0.018
Zr	0.036	0.05	0.026	0.058	0.039	−0.03
Al	0.023	0.056	0.02	0.074	−2.09*	0.032
O	−0.59*	−6.85*	0.01	−1.24*	0.0001	−28.3*
C	−0.006	0.01	−0.00002	0.017	−21.3*	0.03

*Calculated from the experimental data given by Ref. 10.

where its left-hand side, being called solubility function (F), consists only of the weight percentages of the solutes coming from the crucible materials entering into the melt. Similar functions defined for other types of crucibles are summarized in Table VII. Their values being experimentally determined are compared with the quantities obtained from evaluation of the right-hand-side terms of Eq. [12] in Table VIII.

The terms in the right-hand side of Eq. [3] include the standard Gibbs free energy change of the decomposition/dissolution reaction, the temperature, the composition of the titanium present in the melt, and the activity of the base material present in the crucible (for example, ZrO_2). The activities of the base materials of the crucible are assumed equal to their mole fraction. The values for the standard Gibbs free energy changes of the reactions are given in Table III and the temperature is 1723 K. Based on these data and the empirical values of the solutes coming from the crucible being determined by the PIXE Method (Table II), the terms on the right- and left-hand side of Eq. [3] can be calculated. The results are compared in Table VIII. The negative numbers obtained for zirconia- and alumina-based crucibles as compared to the positive ones for SiC-based crucibles are due to both positive sign of the standard Gibbs free energy changes of the zirconia and alumina decomposition reactions as compared to the negative standard Gibbs free energy changes of the SiC decomposition reaction shown in Table III. These signs do not, however, have any special significance besides their resemblance with the sign of the experimentally obtained terms, which might indicate the extent to which the system may approach the equilibrium conditions.

These results are obtained for a Ni-45 wt pct Ti alloy being held inside different crucibles for a period as long as 90 minutes at 1450 °C. A comparison of the equilibrium quantities of the solubility function with the empirical ones, as shown in Table VIII, indicates that except for the commercially pure SiC crucible, the empirical values are greater than the equilibrium ones. The discrepancies seem to be due to the immersion of the undissolved chemical compounds assayed concomitantly with the dissolved solutes by the PIXE method. According to the ternary phase diagram of the Ti-Ni-C system[18] and Ti-Ni-O system[19] the TiC and TiO compounds are produced at the interface layer of the crucibles with the melt by dissolution/chemical reaction of carbon and oxygen with Ni-45 wt pct Ti melt. The melting points of these compounds (1710 °C for TiO and 3065 °C for TiC[20]) are much greater than the temperatures used in this research (1450 °C). So these phases are in solid state at temperatures used in this research.

Table VI. Calculated Second-Order Interaction Parameters in 1 Weight Percent Standard State at 1723 K

J→ / I↓	Ti	Si	Zr	Al	O	C
Ti	0.00032	−0.00085	0.00014	−0.00034	3.51*	−0.00025
Si	−0.00032	0.00045	0.00011	0.00007	16.5*	−0.00017
Zr	0.00019	−0.00006	0.00022	0.00002	−0.00181	−0.00041
Al	−0.00001	0.00009	0.00013	0.0004	0.49*	−0.00191
O	0.04*	5.33*	0.00031	0.17*	0.00035	92.9*
C	0.00009	0.0007	0.00001	0.00143	51.9*	−0.00019

*Calculated from the experimental data given by Ref. 10.

Table VII. Solubility Functions of the Different Crucibles Used for Melting of Ni-45 Wt Pct Ti Alloy at 1723 K

Crucible Type	Calculated Relationship between Dissolved Element of Crucible in NiTi Melt at 1723 K
Recrystallized alumina	$F = (2 \log A + 0.5 A^2 - 3.57 A) + (3 \log O + 0.976 O^2 - 4.188 O)$
Slurry cast alumina	$F = (2 \log A + 0.5 A^2 - 3.57 A) + (3 \log O + 0.976 O^2 - 4.188 O)$
High content zirconia	$F = (\log Z + 0.0003 Z^2 + 0.047 Z) + (2 \log O - 0.001 O^2 + 0.039 O) + (5.33 S^2 - 13.74 S)$
Zircon type A	$F = (\log Z + 0.0003 Z^2 + 0.047 Z) + (2 \log O - 0.001 O^2 + 0.039 O) + (5.33 S^2 - 13.74 S)$
Pure SiC	$F = (\log S + 0.001 S^2 + 0.088 S) + (\log C - 0.0004 C^2 + 0.005 C)$
SiC-Al_2O_3-SiO_2	$F = (\log S + 0.001 S^2 + 0.088 S) + (\log C - 0.0004 C^2 + 0.005 C) + (0.015 A^2 + 0.076 A) + (68.4 O^2 - 33.3 O)$

Table VIII. Equilibrium and Experimental Values of the Solubility Functions Given in Table VII for Crucible Solute Elements Dissolved in Liquid Ni-45 Wt Pct Ti Alloy at 1723 K

Crucible Type	Equilibrium Amounts of Crucible Elements Dissolved in NiTi Melt Determined from Right-Hand Terms of Eq. [12]	Experimental Amounts of Crucible Elements Dissolved in NiTi Melt Determined from Solubility Functions Given in Table VII	Equilibrium to Experimental Ratio
High content zirconia	−76.96	−10.16	7.6
Zircon type A	−79.2	−9.9	8
Recrystallized alumina	−99.8	−7.88	12.7
Slurry cast alumina	−127.4	−7.89	16.2
Pure SiC	6.75	0.5	13.5
SiC-Al_2O_3-SiO_2	6.79	13.92	0.49

According to the equilibrium diagrams of the titanium alloys,[20] solid intermetallic compounds of aluminum and silicon with the titanium can also be formed at temperatures used in this investigation. The amounts of these compounds are not considered, however, in our model, which assumes mere dissolution of the soluble elements into the liquid phase. Gnawing of immiscible solid particles from the crucible and their immersion into the melt can also be a source of increase in the measured impurity contents of the melt. As is indicated by the solubility factor calculations and the chemical analysis results, the crucible materials present in the melt are greater than their solubility limits for five types of crucibles. The melting temperatures of these particles are also, generally, too high to be able to assume them liquefied at the alloy melting temperatures used in this research. Although they remain undissolved solid particles, they can, however, be a source for increase of the impurity contents.

The data given in Table VIII show that for the commercially pure SiC crucible, the dissolution reaction does not reach equilibrium within the experimental periods of the investigation. A prolonged holding time, however, can increase to the quantity of the undesirable contaminants that would enter into the melt. This is consistent with the experimental findings showing the undesirable behavior of the CP SiC crucible. Based on these results, a 90-minute contacting period is not sufficient for dissociation/dissolution reaction to reach equilibrium for commercially pure SiC crucible at 1450 °C.

B. *Sensitivity Analysis*

In order to increase the accuracy of the calculations, both first- and second-order interaction parameters were considered in this study. The influence of the second-order interaction parameters, however, may seem to be negligible due especially to the weight percent standard states being used here. The sensitivity of the final results to the second-order interaction parameters was, therefore, investigated by calculating the effect of the interaction parameters on the solubility functions evaluated for different refractory crucibles.

Substituting the interaction parameter r_O^{Si} into the solubility function (F) of the high content zirconia crucible resulted in, for example, the following introductory correlation:

$$F = (\log Z + 0.00034 Z^2 + 0.0471 Z) + (2 \log O - 0.0011 O^2 + 0.0392 O) + [(r_O^{Si} - 0.00006) S^2 - 13.74 S] \quad [13]$$

Substitution of zirconium, oxygen, and silicon concentrations (given in Table II) into Eq. [13] results in formation of Eq. [14] for high content zirconia and Eq. [15] for SiC-Al_2O_3-SiO_2 crucible:

$$F = 0.83\, r_O^{Si} - 14.58 \quad [14]$$

$$F = 0.524\, r_C^{O} - 14.55 \quad [15]$$

By substituting the interaction parameters $(r_O^{Si})_0 = 5.3358$ and $(r_C^O)_0 = 51.8846$ (Table VI) into Eqs. [14] and [15], the same values as those given in Table VIII are obtained for the solubility functions of the crucibles. The corresponding value of the solubility functions $F_0 = -10.156$ and $F_0 = 12.637$ are obtained for high content zirconia and SiC-Al_2O_3-SiO_2 crucibles, respectively. The subscript 0 is added to the preceding terms in order to specify their fixed amounts as compared to their possible variable numbers.

Solubility function variations defined by $\left(\Delta_1 = \frac{F - F_0}{F_0} \times 100\right)$ are determined as a function of the corresponding second-order interaction parameter change $\left(\Delta_2 = \frac{r_O^{Si} - (r_O^{Si})_0}{(r_O^{Si})_0} \times 100\right)$. Substituting these definitions into Eq. [14] yields

$$\left(\frac{F + 10.156}{-10.156} \times 100\right) \times \frac{-10.156}{100} - 10.156 = 0.83 \times \left[\left(\frac{r_O^{Si} - 5.33}{5.33} \times 100\right) \times \frac{5.33}{100} + 5.33\right] - 14.587$$

or

$$\left(\frac{F + 10.156}{-10.156} \times 100\right) = -0.435 \times \left[\left(\frac{r_O^{Si} - 5.33}{5.33} \times 100\right)\right.$$

which can be simplified to

$$\Delta_1 = -0.435\Delta_2 \quad [16]$$

for high content zirconia crucible and

$$\Delta_1 = 2.16\Delta_2 \quad [17]$$

for SiC-Al_2O_3-SiO_2 crucible.

Figure 5 illustrates the variation of Δ_1 against Δ_2 for high content zirconia and SiC-Al_2O_3-SiO_2 type crucibles. As is seen from the figure, the influence of the second-order interaction parameters is quite substantial and in no way can be considered negligible. In high content zirconia crucible, for example, a 20 pct change in the second-order interaction parameter results in an −8.7 pct change in the solubility function. A similar change for the SiC-Al_2O_3-SiO_2 type crucible is 43.2 pct. These changes show that the elimination of the second-order interaction parameters from the thermodynamic calculations may result in the imposition of a substantial error in the eventual conclusions. Because of the high sensitivity of the thermodynamic data to the second-order interaction parameters, we chose to evaluate the amounts of the pertinent parameters and take them into consideration for reduction of possible errors in the equilibrium calculations.

C. *Scale-up Issues*

Only experimental and thermodynamics analyses of the reactions occurring between the melt and the crucible were considered in this article. Parameters related to the kinetics of the reactions such as bulk liquid volume and crucible-melt interfacial area were also of importance to be evaluated for a scaling-up exercise of the alloy making operation. They do not lie, however, within the scope of this investigation. For a scaling-up exercise, it is of course necessary to take the rate processes into consideration, in detail. The thermodynamics information provided in this research of course can be of help to the design engineer to make an appropriate selection of the crucible and the melting conditions.

Alumina and silicon carbide crucibles are not, for example, suitable for NiTi melting operation because they interact with the melt and cause a sharp rise of the hardness of the eventually produced sample. Previous investigators have used graphite crucibles for melting of the NiTi alloys.[21,22] No comprehensive work, however, has been reported on interactions of other crucibles with the melt. Graphite crucibles, although widely used for NiTi melting operation, have a drawback related to their adding of carbon to the melt. A combination of the semiempirical findings together with the thermodynamics, kinetics, and rate law equations thus can help the design engineers to evaluate the optimum up to the scale NiTi alloy production systems of interest.

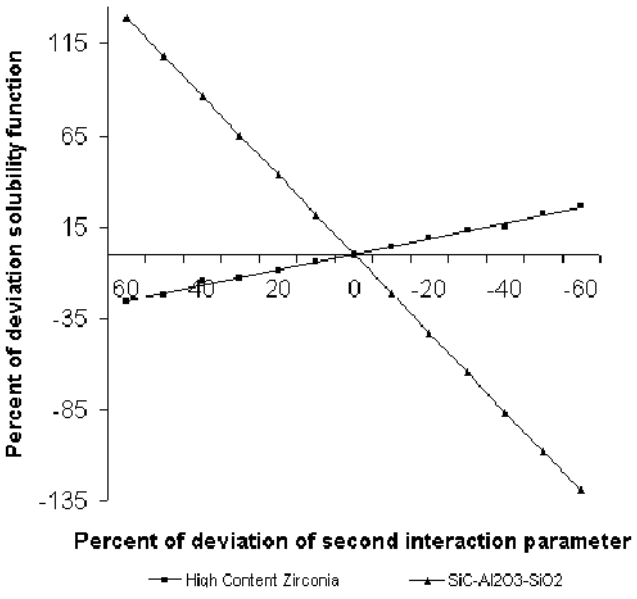

Fig. 5—Curves of percentage of deviation of solubility function *vs* the deviation of second interaction parameter.

IV. CONCLUSIONS

1. The relative stability of the refractory materials can be obtained from the average hardness, SEM image, and chemical analysis by PIXE method. These experiments provide semiquantitative evaluation of the relative stability of the refractory materials.
2. All Al_2O_3-, SiC-, and ZrO_2-based crucibles used in this study reacted with Ni-45 wt pct Ti alloy first melted and then being held at 1450 °C for 90 minutes. The reactions resulted in a hardness increase of the solidified specimens.
3. High content zirconia crucibles had minimum interaction with the melt and commercially pure SiC crucibles had maximum interaction with it.
4. According to visual observations, chemical analysis with the PIXE method, and the average hardness data obtained from the solidified Ni-45 wt pct Ti specimens, the refractory crucibles could be sorted in sequence of increasing stability as CP SiC → SiC-Al_2O_3-SiO_2 → slurry cast alumina → recrystallized alumina → zircon type A → high content zirconia.
5. Negligible amounts of zirconium dissolved in the Ni-45 wt pct Ti melts indicate that an oxygen deficient zirconia crucible with a suitable stabilizer (like titanium) would best suit the melting process for this alloy.
6. Using a quasi-chemical model for determination of the thermodynamic quantities assisted us to evaluate the first- and second-order interaction parameters of the dissolved elements of the crucibles into the Ni-45 wt pct Ti alloy melts. According to these data, the relationships between the equilibrium compositions and the melting conditions could be investigated.
7. Sensitivity analysis was made to determine the effect of the second-order interaction parameters on the amounts of the solubility function evaluated for equilibrium conditions. It was seen that the calculation results are quite

sensitive to the second-order interaction parameters and their negligence causes considerable errors in the theoretical calculations.

8. Thermodynamic treatment of the reactions occurring between the crucible and the melt showed that except for the commercially pure SiC crucible, the measured amounts of the crucible contaminants are greater than the theoretical ones. This finding was attributed to the scuffing of the crucible particles and the formation and scattering of such chemical species as TiC and TiO and the intermetallic compounds of Ti, Al, Si, etc. into the melt.

ACKNOWLEDGMENT

The authors thank Professor Alexander Stomakhin, Moscow State Institute of Steel and Alloys, for his useful guidance and discussions.

REFERENCES

1. *Material Properties Handbook: Titanium Handbook*, T.W. Duering, ed., ASM, Metals Park, OH, 1994.
2. C. Berthold, C. Weber, William M. Thompson, Hans O. Bielstein, and Murray A. Schwartz: *J. Am. Ceram. Soc*., 1975, vol. 40, pp. 363-73.
3. M. Garfinkle and H.M. Davis: *Trans. ASM*, 1965, vol. 58, pp. 520-30.
4. D.R. Schuyler and J.A. Petrusha: *Casting of Low Melting Titanium Alloys*, Vacuum Metallurgy, Science Press, Princeton, NJ, 1977, pp. 475-503.
5. R.L. Saha, T.K. Nandy, R.D.K. Misra, and K.T. Jacob: *Metall. Trans. B*, 1990, vol. 21B, pp. 559-66.
6. J.P. Kuang, R.A. Harding and J. Campbell: *Mater. Sci. Technol*., 2001, vol. 16, pp. 1007-16.
7. *Metals Handbook, Casting*, 9th ed. D.M. Stefanescu, ed., ASM, Metals Park, OH, 1988, vol. 15.
8. S.K. Sadrnezhaad: *Heat and Motion in Materials*, Foreign Ministry Press, Tehran, 1999.
9. O. Kubachewski and C.B. Alcock: *Metallurgical Thermochemistry*, Pergamon Press, msford, NJ, 1979.
10. V. Grigorian L. Belyanchikov, and A. Stomakhin: *Theoretical Principles of Electrical Steel Making*, Mir Publishers, Moscow, 1983.
11. S. Badakhshan Raz: Masters Thesis, Sharif University of Technology, Tehran, 2002 (In Persian).
12. David W. Richardson: *Engineering, Properties Processing and Use in Design*, Marcel Dekker Inc., New York, NY, 1992.
13. Ahmad Monshi: *Ceramics and Refractory Materials*, 3rd ed. Jahad Daneshgahi Publications, Isfahan, Iran, 1996.
14. C.H. Lupis and J.F. Elliot: *Acta Metall*., 1966, vol. 14, pp. 529-38.
15. C.H. Lupis and J.F. Elliot: *Acta Metall*., 1966, vol. 14, pp. 1019-32.
16. F.D. Richardson: *Physical Chemistry of Melts in Metallurgy*, vol. 1. Academic Press, New York, NY, 1974.
17. H. Ashori: *Crystallography*, Jahad Daneshgahi Publications, Isfahan, Iran, 1989.
18. E.R. Stover and J. Wulff: *Trans. TMS-AIME*, 1959, vol. 215, pp. 127-36.
19. E.K. Nolchanova: *Diagram of Titanium Alloys*, Israel Program for Scientific Translations, Jerusalem, 1965.
20. *Desk Hand Book, Phase Diagrams for Binary Alloys*, Hiroaki Okamoto, ed., ASM, Metals Park, OH, 2000.
21. J. Frenzel, Z. Zhang, K. Neuking, and G. Eggeler: *J. Alloys Compounds*, 2004, vol. 385, pp. 214-23.
22. M.H. Wu: *Proc. Int. Conf. on Shape Memory and Superelastic Technologies*, *Trans. Tech.*, Kuming, China, 2001, pp. 285-92.